Molecular beam experiments on the sticking and accommodation of molecular hydrogen on a low-temperature substrate[a]

T. R. Govers,[b] L. Mattera,[c] and G. Scoles[d]

Guelph-Waterloo Center for Graduate Work in Chemistry and Department of Chemistry, University of Waterloo, Waterloo, Ontario N2L 3G1, Canada

Molecular beams, microcalorimetry, and mass spectrometry are used to study the physisorption kinetics of H_2 and D_2 molecules on a low temperature substrate. The energy transferred to the surface of a liquid-helium cooled bolometer by an incident room temperature beam of H_2 and D_2, and the number density of the scattered molecules are measured. The sticking coefficient S and the accommodation coefficient α are obtained as a function of N, the surface coverage by H_2 or D_2. For both isotopes, S and α depend strongly on N. $S(H_2)$ changes from 0.07 ± 0.05 to 0.80 ± 0.02 and $\alpha(H_2)$ from 0.31 ± 0.07 to 0.97 ± 0.01 as N increases from $\simeq 0$ to 3×10^{15} molecule cm^{-2}. In the same coverage range, $S(D_2)$ changes from 0.25 ± 0.05 to 0.92 ± 0.04 and $\alpha(D_2)$ from 0.3 ± 0.1 to 0.975 ± 0.025.

I. INTRODUCTION

The recombination of atomic hydrogen on low temperature surfaces is of fundamental importance because it represents one of the simplest heterogenous chemical reactions. It is of astrophysical interest because it is presently thought to constitute the main mechanism for formation of molecular hydrogen in interstellar space,[1-4] and it is also relevant to the possibility of forming stable phases of polarized single atoms,[5,6] which could conceivably be used to store large quantities of energy in small physical volumes.[5-7]

Following the first molecular beam study of heterogeneous H-atom recombination by Brackmann and Fite,[7] Marenco *et al.*[8] and Schutte *et al.*[9] studied this reaction under improved vacuum conditions by measuring the energy released by a beam of H (or H_2) when it impinges on the surface of a liquid-helium cooled bolometer which serves both as a beam detector and as a catalytic substrate for H-atom recombination. They found that the fate of the incoming H is strongly affected by the amount of molecular H_2 previously adsorbed on the surface.

The purpose of the study reported in the present contribution and in a subsequent paper[10] is to provide additional experimental data aimed at specifying the main parameters governing the overall recombination rate: adsorption energies, accommodation and sticking coefficients, and reaction probabilities of adsorbed atoms. Because these parameters depend strongly on H_2 coverage and because certain aspects relevant to the physisorption of molecular hydrogen should find their analog in the behavior of atomic hydrogen, we first undertook a number of experiments on molecular H_2 and D_2. The results of this work are the subject of the present paper, while those pertaining to the adsorption and recombination of atomic hydrogen are discussed elsewhere.[10]

As in the experiments by the Genova group,[8,9] effusive room temperature beams of H_2 or D_2 were made to impinge on the surface of a liquid-helium cooled bolometer (microcalorimeter), whose output signal is a measure of the total energy (kinetic, internal, and adsorption energy) released to its surface by the incoming beam. While in the work of Schutte *et al.*[9] a second bolometer was used to detect the molecules reflected by the first surface, the present experiment employed a rotatable quadrupole mass spectrometer for this purpose.

It should be mentioned from the outset that the host surface used in this work is not crystallographically well defined. During cooldown of the liquid-helium cryostat which supports it, the bolometer (a doped Si slab) becomes covered with a cryodeposit of background gas consisting mainly of frozen air, water ice, and a small amount of hydrocarbons. No attempt was made to free the bolometer surface from this background frost: The excellent reproducibility of the measurements over periods of more than a year and the close similarity with those obtained at Genova indicate that for the present purpose the surface thus obtained is reproducible and stable. The key factor to be controlled is the amount of molecular hydrogen present on the surface. It can be removed by raising the bolometer temperature, while it can be deposited in reproducible amounts using a beam of H_2 or D_2.

In the following paragraphs we shall first give a brief description of the apparatus which was constructed to perform the measurements (Sec. II). The experimental data are presented and analysed in Sec. III and the discussion of the results is given in Sec. IV.
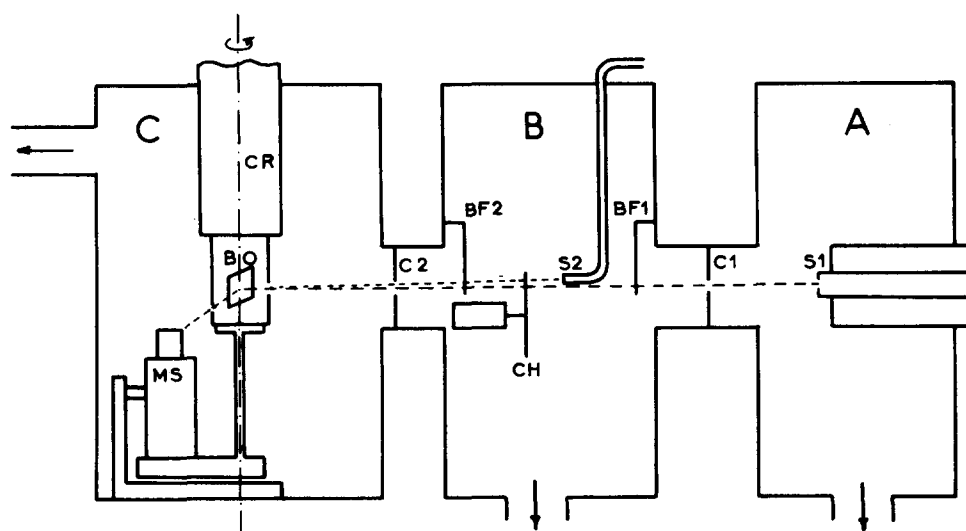
FIG. 1. Schematic drawing of the apparatus. A, B, and C: vacuum chambers; S1, S2: beam sources; C_1, C_2: collimators; BF1, BF2: beam flags; CH: beam chopper; BO: bolometer; MS: mass spectrometer; CR: cryostat.

II. APPARATUS

The apparatus is shown schematically in Fig. 1. Its main constituents are a molecular beam source, a liquid-helium cooled bolometer, which serves as a microcalorimetric beam detector, and a quadrupole mass spectrometer MS which detects the beam particles reflected by the bolometer surface.

The beam source S_1 is located in chamber A, which is evacuated by a 4000 l/s oil diffusion pump. The source pressure (typically 2 Torr) was kept sufficiently low to ensure a linear variation of beam intensity with source pressure. The latter was measured with a Validyne diaphragm gauge, calibrated against a McLeod gauge.

The beam enters chamber B through the collimator C_1. Chamber B is evacuated by a water-baffled oil diffusion pump and acts as a differential pumping stage with an effective pumping speed of about 2000 l/s. It contains a secondary beam source S_2 (which is only used in the experiments with atomic hydrogen[10]), two beam flags, and a chopper which modulates the beam with a 50% duty cycle at a frequency of 23 Hz. The beam finally enters chamber C through a collimator C_2.

Chamber C is evacuated by a liquid-nitrogen baffled oil diffusion pump with an effective pumping speed of a about 1200 l/s, and contains the bolometer and mass spectrometer.

The bolometer is mounted vertically on the bottom of the reservoir of a liquid-helium cryostat. Its surface normal makes an angle $\theta_i = 45°$ with respect to the (horizontal) beam axis. The bolometer is surrounded by liquid helium cooled surfaces, except for the two apertures (total area = 9.5 mm^2, total solid angle 1.3 $\times 10^{-2}$ sr) which serve to admit the beam and to detect reflected molecules with the mass spectrometer. This provides the bolometer with an UHV environment of $< 10^{-11}$ Torr (for a bath temperature < 4 K), while the outer liquid-nitrogen cooled shroud of the cryostat acts as a cryopump for chamber C. During the experiments, the background pressure in C is $\simeq 10^{-8}$ Torr (mainly

hydrogen), and the resulting contamination of the bolometer surface amounts to $< 6 \times 10^{10}$ molecule cm^{-2} s^{-1}, which means that the buildup of one monolayer requires about 300 min.

The beam intensity at the bolometer surface, averaged over the modulation period, is typically 2×10^{14} molecule cm^{-2} s^{-1}, and the measuring time a few minutes. It follows that the modification of the surface coverage during the measurements is almost entirely due to the incident beam particles.

The bolometer is a doped Si slab (2.1×4.1×0.3 mm^3) which detects the power dissipated by the incident beam as outlined in Ref. 11. Its surface was polished to a mirror finish by means of a Teflon-coated disk. The area exposed to the incident beam measures 4.7 mm^2. In the present mounting, the noise equivalent power at a temperature of 3 K is 10^{-9} W Hz$^{-1/2}$ and the response time about 10^{-3} s. The bolometer temperature T_s is regulated by controlling the pressure over the liquid He bath and the bias current. It is determined within ~ 0.05 K by measuring the static bolometer resistance, which varies by about 1 kΩ per degree at 3 K. Experiments were performed for $3 \leq T_s \leq 10$ K, but only the 3 K results will be discussed in detail.

As indicated in the Introduction, hydrogen molecules accumulated on the surface during the measurements are evaporated by raising the bolometer temperature to ~ 30 K. This is achieved by increasing the bias current to ~ 40 mA during 30 s, ensuring desorption of all molecules (and in particular H_2 and D_2) with surface binding energies $E/k < 1000$ K. This restores the surface composition to a cryodeposit which, for the present measurements, is indistinguishable from the cryodeposit formed during the initial cooldown of the cryostat.

The mass spectrometer is a commercial quadrupole instrument (Extranuclear). It can be rotated in the horizontal plane which contains the incident beam axis to detect particles emitted from the bolometer surface as a function of the angle θ_f to the surface normal. The

angular distribution was found to follow a $\cos\theta_f$ dependence under all experimental conditions. The measurements reported here were obtained at $\theta_i = \theta_f = 45°$.

The MS ionizer has an open structure, ensuring that the incident particles make a single pass through the ionizing region. The MS signal is therefore a measure of the density of the detected particles, i.e., it measures the ratio (flux/speed) of the molecules emitted by the bolometer.[7]

The bolometer and mass spectrometer signals are fed into lock-in amplifiers tuned to the beam chopping frequency. With a lock-in time constant of 0.1–0.3 s, compatible with the rate of change of the observed signals, that due to the bolometer has a sufficiently high signal to noise ratio to be chart recorded directly. The output from the MS lock in, however, requires treatment by a signal averager (Ubiquitous UC 201 C Correlator) to achieve an acceptable S/N while preserving a $\leqslant 0.3$ s response time.

A final comment concerns the effective surface temperature. The MS ionizer is surrounded by a liquid-N_2 cooled shield to reduce the thermal radiation on the bolometer. Even so, the measured bolometer temperature rises by ~ 0.2 K when the ionizer is turned on. It was verified, however, that the beam signals measured with the bolometer are the same whether the MS ionizer is on or off, provided that the measured bolometer temperature is kept the same by adjusting the pressure over the liquid-He bath. This indicates that there is no significant difference between the measured bulk temperature and the temperature of the surface layers adsorbed on the bolometer.

III. EXPERIMENTAL DATA AND THEIR ANALYSIS

A. Experimental data

In Fig. 2 we show the bolometer and MS signals observed when a constant-intensity H_2 beam is made to impinge on the initially H_2-free bolometer surface. The data were obtained at $T_s = 3$ K and represent the average of 50 individual measurements. In each of these, the bolometer was first "cleaned" by evaporating previously deposited H_2 as outlined in Sec. II, while the beam flag was kept closed. Once T_s was restored to 3 K, the beam flag was opened ($t = 0$) and the two lock-in signals were measured simultaneously. The bolometer signal was chart recorded for each measurement. Its excellent reproducibility (within $< 3\%$) served to verify the reproducibility of the surface conditions. The MS signal was fed into the signal averager, and its output was recorded at the end of the 50 measurements (total measuring time $\simeq 2$ h).

The bolometer signal, which varies linearly with the incident beam intensity (source pressure), is expressed as the average energy released per incident molecule by means of a calibration discussed in Sec. III. C below. The MS signal is given in dimensionless units (cf. Sec. III. B) by normalization to the signal which would be observed if all particles incident on the bolometer were to enter the MS ionizer at the same speed as the primary beam particles ($q > 1$ means that the average speed of
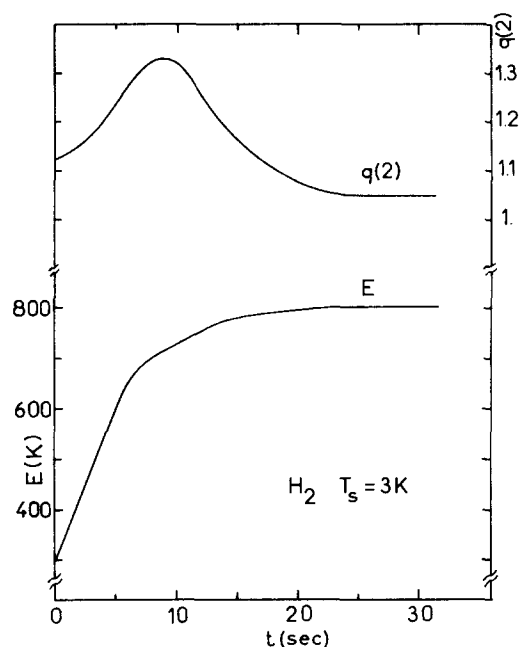

FIG. 2. Results obtained for a $(2.0 \times 10^{14}\ \mathrm{mol/cm^2\,s})$ H_2 beam impinging on a surface initially free of H_2, at $T_s = 3$ K; bolometer (E) and mass spectrometer (q_2) signals as a function of the beam exposure time. For the $q_2(t)$ and the $E(t)$ scales, see Secs. III. B and III. C.

the reflected molecules is lower than that of those in the primary beam, resulting in a higher ionization probability).

Figure 3 shows the data obtained in the same manner with D_2. Experiments were also conducted at a surface temperature of $T_s = 10$ K. The time behavior observed for the bolometer signal was similar to that reported by the Genova group[9]: With the same H_2 beam intensity as in the 3 K experiments, the signal was found to level off at an exposure time close to the first "break" observed at $t \simeq 8$ s in Fig. 2. In the 10 K experiments the higher cryostat temperature decreases the pumping speed for the hydrogen brought in by the beam, resulting in higher background pressures and a more than tenfold lower S/N on the MS signal. Given the limited holding time of the cryostat (6–8 h), it was not possible to obtain a sufficiently high S/N to allow a quantitative interpretation of the MS data. Qualitatively, however, the results do confirm the interpretation of the 3 K results.

Before interpreting the time dependence of the signals illustrated by Figs. 2 and 3, we recall that the arrival rate at the bolometer surface due to the impinging beam molecules is much larger than that due to the inward diffusion of the background gas (mainly hydrogen during the experiments) surrounding the cryostat. The observed signal changes must therefore be due to a progressive coverage of the bolometer by molecular hydrogen deposited by the beam. Indeed, the time scale of the data of Figs. 2 and 3 is found to be inversely proportional to the beam intensity. If the beam is temporarily interrupted, the signals observed when the beam flag is opened again are the same as those registered before it was closed. It was also verified that attenuating the
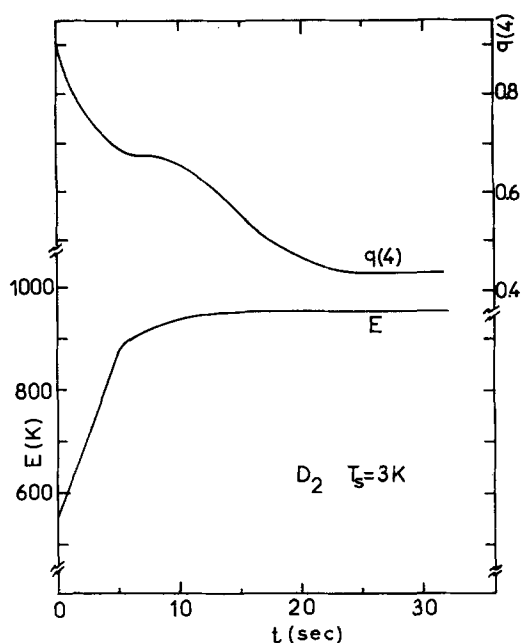
FIG. 3. Same as in Fig. 2, for a D_2 beam of $(1.2 \times 10^{14} \text{mol}/ \text{cm}^2 \text{s})$.

beam by interposing a 40% transparent screen reduces the signals to the same 40% level, irrespective of the beam exposure time, i.e., irrespective of the surface coverage.

These observations indicate that the amount of molecular hydrogen adsorbed on the bolometer surface does not affect the linear dependence of the bolometer signal on beam intensity, but that it changes the average amount of energy released to the surface per incident molecule. The signal recorded by the mass spectrometer varies because the fraction of the beam molecules scattered towards this detector depends on the bolometer coverage and/or because their velocity changes.

B. Definitions

To interpret the data of Figs. 2 and 3 quantitatively, we shall distinguish between beam molecules which "stick" on the bolometer surface and those which are "reflected." The fraction S of the molecules which stick are those which become thermalized to the surface temperature T_s, liberating the incident kinetic energy E_k, the available internal energy E_{int}, and the difference $(\epsilon - kT_s)$, where ϵ is the binding energy. With values $\epsilon/k \geqslant 95$ K, appropriate to the present experiments, the residence time of those molecules is $\geqslant 3$ s, i.e., much longer than the beam modulation half-period $(3.7 \times 10^{-3}$ s). Upon leaving the surface they will have lost the phase relationship with the incident beam, so that they will not contribute to the MS lock-in signal. However, the energy transfer to the surface occurs on a time scale much shorter than 10^{-3} s, so that the energy liberated by the molecules which stick will contribute to the bolometer lock-in signal. The reflected beam particles [fraction $(1 - S)$] are those whose residence time on the surface is small compared to the beam modulation time. These are the molecules responsible

for the MS lock-in signal, since they preserve the phase of the incoming beam.[7]

Molecules which do not stick are taken to leave the surface with an average translational energy of $2kT_f$ and are characterized by the accommodation coefficient α:

$$\alpha \equiv \frac{T - T_f}{T - T_s} \quad , \tag{3.1}$$

where T is the temperature of the source and T_s that of the surface. Assuming that the fraction of the internal energy transferred to the surface can be approximated by α,[12] the average energy transferred to the bolometer surface per incident molecule is

$$E = S(E_k + E_{int} + \epsilon - kT_s)$$

$$+ (1 - S)\alpha (E_k - 2kT_s + E_{int}) \, . \tag{3.2}$$

At any given beam intensity, the bolometer signal is proportional to E, and changes in signal result from changes in S, ϵ, and α. For a source temperature T (which was 293 K in all experiments), the average kinetic energy per beam particle is $2kT$. The internal energy for $T = 293$ K is essentially rotational energy; if we assume that no ortho- to parahydrogen conversion takes place on the surface, the available rotational energy[13] is 141 K for H_2 and 251 K for D_2.[14] We thus obtain, for H_2,

$$E = (724 + \epsilon)S + 721(1 - S)\alpha, \tag{3.3}$$

and for D_2,

$$E = (834 + \epsilon)S + 831(1 - S)\alpha. \tag{3.4}$$

According to the above definitions, the signal due to reflected particles (mass m) measured with the mass spectrometer $Q_{f,m}$ can be written as

$$Q_{f,m} = g_m \omega \Omega_B \phi (1 - S)(4kT_f/m)^{-1/2} \quad , \tag{3.5}$$

where $\phi = \phi(p)$ is the beam intensity per unit solid angle at a source pressure p, Ω_B the solid angle subtended by the bolometer at the beam source, g_m the mass dependent detection efficiency (lock-in signal at unit density in the ionizer region), and ω a geometrical factor which gives the fraction of the molecules reflected from the bolometer surface which enter the mass spectrometer ionizer. Once it has been established that $Q_{f,m}$ follows a $\cos\theta_f$ dependence, ω can be calculated from the geometry of the experimental setup. The $T_f^{-1/2}$ dependence results from the fact that the mass spectrometer is a density (=flux/speed) detector.

To eliminate the detection efficiency g_m from Eq. (3.5), we carried out a separate set of experiments in which the bolometer was removed and the mass spectrometer made to intercept the incident beam at various source pressures p. In these experiments the signal is

$$Q_{0,m} = g_m \Omega_q \phi (4kT/m)^{-1/2} \quad , \tag{3.6}$$

where Ω_q is the solid angle through which the beam particles enter the ionizer. Knowing ω, Ω_B, and Ω_q, values of $Q_{f,m}$ and $Q_{0,m}$ obtained at the same source pressure could thus be compared to yield the reduced signal $q(m)$, which is the quantity plotted in Figs. 2 and 3:

$$q(m) \equiv Q_{f,m} \; \frac{1}{\omega Q_{0,m}} \times \frac{\Omega_q}{\Omega_B} = (1-S)\,(T/T_f)^{1/2} \quad . \quad (3.7)$$

Defining

$$\gamma \equiv 1 - T_s/T, \tag{3.8}$$

the measurement of the reduced mass spectrometer signal thus establishes a relation between α and S through [Eqs. (3.1), (3.7), and (3.8)]

$$q(m) = (1-S)\,(1-\alpha\gamma)^{-1/2} \quad . \tag{3.9}$$

C. Calibration of the bolometer signal

To calibrate the bolometer response, i.e., to express the measured bolometer signal at a given arrival rate of beam molecules in units of E, the average energy transferred per incident particle, we made use of the results found by Schutte et al. in their two-bolometers experiment on H_2 (Fig. 5 of Ref. 9). The first bolometer B_1 intercepts the primary beam and is initially (almost) H_2 free, while B_2, which is saturated with H_2, detects molecules which do not stick on B_1. At temperatures below 4.25 K, the signal on B_1 varies in a manner similar to that shown in Fig. 2, i.e., it eventually reaches a constant value $IB_{1\infty}$, while IB_2 decreases to a constant value $IB_{2\infty}$. It is found that $IB_{1\infty}$ amounts to 97% of the sum $(IB_{1\infty} + IB_{2\infty})$, where $IB_{2\infty}$ has been corrected for the finite acceptance angle and the different sensitivity of the second bolometer. As shown in the Appendix, this observation is compatible with our results only if those molecules which do not stick on the first bolometer do so on the second (as already assumed by Schutte et al.[9]). This means that the sum $(IB_{1\infty} + IB_{2\infty})$ represents a signal corresponding to unit overall sticking coefficient, i.e., $E_{1\infty} + E_{2\infty} = (724 + \epsilon_\infty)$ so that $E_{1\infty} = 0.97(724 + \epsilon_\infty)$, where the subscript ∞ refers to asymptotic (large) H_2 coverage. Taking into account the relative beam intensities for Ref. 9 and the present experiments, this regime applies to exposure times of ≥ 30 s in Fig. 2.

Assuming that the adsorption characteristics of our bolometer and those of Schutte et al. are identical for large H_2 coverage, we thus identify our bolometer signal IB_∞ at $t \geq 30$ s (Fig. 2) with an energy release per incident molecule

$$E_\infty = 0.97(724 + \epsilon_\infty) \quad . \tag{3.10}$$

This calibrates the signal once ϵ_∞ can be established.

The value adopted for ϵ_∞ was 103 K, the sublimation energy ϵ_s of H_2 at 3 K.[15] The reasons for taking $\epsilon_\infty = \epsilon_s$ is as follows: The observation that at sufficiently long exposure times the signal on both bolometers in the experiments of Schutte et al.,[9] and of the bolometer and the mass spectrometer in the present work, remain con-

stant in time, can mean either that H_2 is no longer accumulating on the surface or that further accumulation does not affect α, S, and ϵ. The first situation occurs when the evaporation rate from the uppermost H_2 layer becomes equal to the arrival rate of beam molecules. With the beam intensities used here and in Ref. 9, this is possible when the average residence time of molecules in the uppermost layer τ shortens to $\simeq 5$ s. With $\tau = \tau_0 \, e^{\epsilon_\infty/kT_s}$, $\tau_0 \simeq 10^{-13}$ s, and $T_s = 3$ K, this leads to the requirement $\epsilon_\infty \simeq 95$ K if we neglect possible evaporation of the uppermost layer due to thermal radiation. This seems reasonable in view of the comments made at the end of Sec. II. If, on the other hand, hydrogen keeps accumulating in the asymptotic regime, the binding energy must become equal to ϵ_s at long exposure times, justifying the choice $\epsilon_\infty = \epsilon_s$ when there is no more measurable change in the bolometer and mass spectrometer signals. We shall see in Sec. IV. A that taking $\epsilon_\infty = \epsilon_s$ provides internal consistency between the analysis of the H_2 and D_2 results. In any event, changing ϵ_∞ from 103 to 115 or 95 K introduces an uncertainty in the bolometer calibration [see Eq. (3.10)] of $\simeq 1\%$. The effect due to changes in the choice of ϵ_∞ on the values of α_∞ and S_∞ deduced from our measurements is discussed in Sec. IV. A.

D. Calculation of S and α for H_2

Having calibrated the bolometer signal, the simultaneous measurements of the bolometer and reduced quadrupole signals as a function of t, the exposure time to the H_2 beam, provides us with the following pair of equations:

$$E = (724 + \epsilon)S + 721(1-S)\alpha \quad , \tag{3.3}$$

$$q = (1-S)\,(1-\alpha\gamma)^{-1/2} \quad . \tag{3.9}$$

Obviously, the measurements of $E(t)$ and $q(t)$ (Fig. 2) are not sufficient to determine the three variables $\epsilon(t)$, $\alpha(t)$, and $S(t)$. Incorporating the results of the two-bolometers experiments of Schutte et al.[9] would provide a third independent equation. While this is reasonable for large H_2 coverage (large t)—and this is what we have done in the preceding section—the experimental conditions in the two investigations were not sufficiently similar to warrant this procedure at short exposure times, because there the temporal variation of the measurements depends critically on the incident beam intensity, the "cleanliness" of the surface at $t=0$, and the surface temperature.

We have therefore deduced S and α from our measurements by treating ϵ as an adjustable parameter. The results of Fig. 2 were analyzed at 17 values of the beam exposure time t_i spaced (except for $t_{17} = 30$ s) by a constant interval $\Delta t = 1.6$ s, using the following form for $\epsilon(t_i)$:

$$\epsilon(t_i) = \begin{cases} \epsilon_0 & i = 1, n_1 \\ \epsilon_\infty + (\epsilon_0 - \epsilon_\infty)\exp\{-[t_i - (n_1 - 1)\Delta t]^2/2(n_2 - n_1)^2 \Delta t^2\}, & i = n_1, 16 \\ \epsilon_\infty & i = 17 \end{cases} \tag{3.11}$$
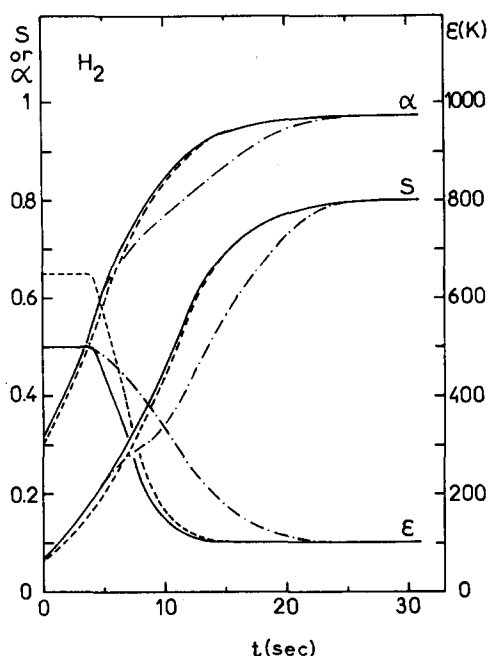
FIG. 4. Influence of $\epsilon(t)$ [Eq. (3.11)] on the values of S and α calculated from the data reported in Fig. 2: $\epsilon_0 = 500$ K, $\epsilon_\infty = 103$ K, $n_1 = 3$, $n_2 = 5$ (—); $\epsilon_0 = 650$ K, $\epsilon_\infty = 103$ K, $n_1 = 3$, $n_2 = 5$ (- -); $\epsilon_0 = 500$ K, $\epsilon_\infty = 103$ K, $n_1 = 3$, $n_2 = 7$ (- · - ·).

This functional form, illustrated in Fig. 4, reproduces the requirement that ϵ should have a value which is essentially constant both at short times, where the surface coverage is small, and at large times, where the observed signals no longer change (cf. Sec. III. C). The second line in Eq. (3.11) provides a computationally convenient transition between the two plateaus. The solid line $\epsilon(t)$ in Fig. 4 connects the points calculated for $\epsilon(t_i)$ when one takes $n_1 = 3$, $n_2 = 5$, and $\epsilon_0 = 500$ K, ϵ_∞ being fixed at 103 K (Sec. III. C). At first sight this choice may appear quite arbitrary. In fact, trial calculations show that there is not much leeway in the representation of $\epsilon(t_i)$ if we wish to reproduce our simultaneous measurements of $E(t_i)$ and $q(t_i)$ [Eqs. (3.3) and (3.9)] without introducing discontinuities in dS/dt and $d\alpha/dt$. The latter would give rise to discontinuities in the signal of the second bolometer in the experiments of Schutte et al.,[9] and this is not observed. Considering, for example, the "break" in the bolometer signal observed at $t \simeq 8$ s in Fig. 2, a smoothly increasing S and α require a rather abrupt decrease in ϵ at slightly shorter exposure times. This yields $3 \leqslant n_1 \leqslant 4$, $(n_1 - 1)$ Δt being the length of the initial plateau in ϵ.

The major uncertainty in the representation of $\epsilon(t_i)$ resides in the value of ϵ_0, but the resulting indetermination in S and α is small. This can be seen in Fig. 4 by comparing the results obtained by choosing $\epsilon_0 = 500$ K (solid lines) or $\epsilon_0 = 650$ K (broken lines); in both cases $n_1 = 3$, $n_2 = 5$. The range of possible ϵ_0 values is considered further in Sec. IV. B. The effect of changing n_2 can be seen by comparing the solid curves with the dash–dotted lines, where n_2 was changed from 5 to 7.

E. Calculation of S, α, and ϵ_∞ for D_2

The analysis of the D_2 results reported in Fig. 3 was performed in a manner analogous to that applied to the H_2 data. The bolometer signal was measured relative to that for an H_2 beam of equal incident flux, so that absolute $E(D_2)$ values [Eq. (3.4)] could be obtained using the H_2 calibration discussed above.

IV. DISCUSSION

In the following paragraphs we shall first examine how the values of α and S calculated from the experimental measurements at high (Sec. IV. A) and low (Sec. IV. B) hydrogen coverage depend on the corresponding choice of ϵ, and discuss the possible range of values for ϵ_0.

In Sec. IV. C we summarize our findings regarding the dependence of S, α, and ϵ on the amount of hydrogen adsorbed on the surface and compare these with some published experimental and theoretical data.

A. Choice of ϵ_∞ and uncertainties in α_∞ and S_∞

Table I(a) lists the solutions to Eqs. (3.3) and (3.9) obtained from the measurements of the asymptotic H_2 signals with ϵ_∞ as a parameter. As indicated in Sec. III. C, ϵ_∞ should be close to the sublimation energy of solid H_2 $\epsilon_s(H_2) = 103$ K.[15] It is seen that a $\simeq 10\%$ variation in $\epsilon_\infty(H_2)$ around this value changes α_∞ and S_∞ for H_2 by only $\simeq 1\%$.

A similar variation is obtained for the value of $E_\infty(H_2)$, i.e., the bolometer calibration, which depends on the choice of $\epsilon_\infty(H_2)$ through Eq. (3.10). A 10% uncertainty in the measured value of $q_\infty(H_2) = 1.05$ affects α_∞ and S_∞ by $< 1\%$.

The right-hand side of Table I refers to the asymptotic D_2 data. In this case, α_∞ and S_∞ depend both on $\epsilon_\infty(H_2)$—through the bolometer calibration which determines the absolute value of E_∞—and on $\epsilon_\infty(D_2)$. This

TABLE I. Effect of the choice of ϵ_∞ on the values of E_∞, α_∞, and S_∞.

(a)	H_2			(b)	D_2		
ϵ_∞(K)	E_∞ (K)	α_∞	S_∞	E_∞ (K)	α_∞	S_∞	ϵ_∞ (K)
					0.95	0.893	130
95	794	0.971	0.793	945	0.975	0.918	123
					1.0	0.956	116
					0.95	0.893	139
103	802	0.974	0.801	954	0.975	0.918	133
					1.0	0.956	126
					0.95	0.893	156
115	814	0.978	0.812	969	0.975	0.918	149
					1.0	0.956	141

[a]Values of E_∞, α_∞, and S_∞ for H_2 calculated from Eqs. (3.3), (3.9), and (3.10), with $q_\infty = 1.05$.
[b]Values of E_∞, α_∞, S_∞, and ϵ_∞ for D_2 calculated from Eqs. (3.4) and (3.9) with $q_\infty = 0.44$, after having calibrated the bolometer signal and imposing $\alpha_\infty(H_2) \simeq \alpha_\infty(D_2)$.

TABLE II. Effect of the choice of ϵ_0 on the values of S_0 and α_0 at $t = 0$.[a]

H₂	$q_0 = 1.0_2$ 1.1_2 1.2_2		D₂	$q_0 = 0.8_4$ 0.9_1 0.9_9	
ϵ_0 (K)	α_0	S_0	ϵ_0 (K)	α_0	S_0
	0.26	0.12		0.30	0.29
360	0.32	0.07	400	0.35	0.27
	0.38	0.03		0.40	0.24
	0.25	0.11		0.25	0.28
500	0.32	0.07	550	0.35	0.27
	0.37	0.03		0.38	0.23
	0.24	0.10		0.21	0.26
650	0.31	0.06	720	0.31	0.25
	0.37	0.03		0.35	0.21

[a]The three values reported for each ϵ_0 are calculated to allow for a 10% experimental uncertainty in the reduced MS signals $q_0 (H_2) = 1.1_2$ and $q_0 (D_2) = 0.9_1$.

dependence is slightly stronger than for H_2, but the effect of a 10% variation in either parameter remains $< 10\%$. The effect of a $\simeq 10\%$ uncertainty in the measured $q_\infty (D_2) = 0.44$ is about 1%. Inspection of Table I also shows that fixing $\epsilon_\infty (H_2) = \epsilon_s (H_2) = 103$ K and requiring $\alpha_\infty (D_2) \simeq \alpha_\infty (H_2)$ does yield $\epsilon_\infty (D_2) \simeq \epsilon_s (D_2) = 143$ K,[15] which provides an internal consistency check on our analysis.

B. Choice of ϵ_0 and uncertainties in α_0 and S_0

The range of possible values of ϵ_0, the binding energy on the hydrogen-free bolometer surface, was estimated from published theoretical and experimental results.

If the gas-surface interaction potential $V(z)$ is estimated from the pairwise potential $v_i(z)$ between the two species involved, the well depth D is approximately given by $D \simeq \delta D_i$, where D_i is the potential well depth of $v_i(z)$ and the numerical factor δ ranges from about 4 to 8.[16,17] For the main constituents of the cryodeposit covering the H_2-free bolometer (N_2, O_2, H_2O, ...), the value of δ is not expected to be very different, so that an upper limit to ϵ_0 can be estimated by considering the surface to be covered only by the molecule having the strongest gas-phase interaction with hydrogen. This is the case for H_2O, for which H_2-H_2O molecular beam scattering data give a well depth of 130 K.[18] Lee has measured the binding energy of H_2 on solid H_2O to be 860 K,[19] while the isosteres reported by Yuferov and Busol (Fig. 6 of Ref. 20) yield a value of about 460 K. The theoretical evaluation of Hollenbach and Salpeter[16] gives $\simeq 615$ K when one replaces the gas-phase well depth they used (100 K) by the recent figure of 130 K.[18] On the basis of these results we have adopted an upper limit $\epsilon_0 (H_2) \leq 650$ K. As a lower limit we have taken the value for $\epsilon_0 (H_2) = 360$ K evaluated by Schutte et al.[9] In their $T_s \leq 4.2$ K experiments, the ratio E_∞ / E_0 on the first bolometer is somewhat lower than in ours, pre-

sumably because under initial conditions their surface is not quite as H_2 free as ours. Since the adsorption of H_2 decreases the binding energy, it is reasonable to assume $\epsilon_0 (H_2) \geqslant 360$ K in our experiments.

Bounds to the ϵ_0 range for D_2 were obtained by scaling those used for H_2. Molecular beam experiments on resonant surface scattering by O'Keefe et al.[21] on H_2, D_2/LiF and by Mattera et al.[22] on H_2, $D_2/$graphite show that the lowest adsorption level for D_2 lies $< 8\%$ lower than that for H_2. Adsorption energy measurements by Van Itterbeek et al.[23] for H_2, D_2 on Ag and graphite show similar changes. A comparison of the binding energies computed by Hollenbach for H/H_2O and for H_2/H_2O,[16] which were obtained using the same potential parameters for the two systems, suggests an increase in binding by $\simeq 20\%$ when going from H_2 to D_2/H_2O. On the basis of this information we have taken $\epsilon_0 (D_2) \simeq 1.1 \times \epsilon_0 (H_2)$, i.e., $400 \leqslant \epsilon_0 (D_2) \leqslant 720$ K.

Table II lists the values of α_0 and S_0 obtained by substituting our experimental values of $E_0 (H_2, D_2)$ and $q_0 (H_2, D_2)$ (Figs. 2 and 3) in Eqs. (3.3), (3.4), and (3.9) using ϵ_0 as a parameter within the ranges quoted above. It is seen that α_0 and S_0 depend only weakly on the value of ϵ_0, the major uncertainty being due to the possible experimental error on q_0. The uncertainty in the absolute value of E_0 (i.e., the bolometer calibration) results in an absolute error of < 0.01 for each of $\alpha_0 (H_2, D_2)$ and $S_0 (H_2, D_2)$. We note that accepting the value of $q_0 (D_2) = 0.8$ gives the unrealistic result $\alpha_0 < S_0$, which indicates that the uncertainty of ± 0.1 assigned to the measured q_0 is rather pessimistic.

C. Dependence of α and S on surface coverage by H_2 and D_2

In Figs. 5 and 6 we have summarized our findings on the variation of α and S with beam exposure time, and with H_2 and D_2 coverage. The upper and lower bounds shown account for the sum of the uncertainties in the measurement of the reduced quadrupole signal q and of those due to the variation of the parameters in $\epsilon(t)$ as given in the figure captions. The error on α is conservatively evaluated at an absolute value of about ± 0.07 throughout all measurements, which represents about $\pm 20\%$ at $t = 0$ and $\pm 7\%$ at long exposure times. The value of S is only determined within a factor of 2 at $t = 0$, but this situation rapidly improves to give a $\simeq 30\%$ uncertainty at $S \simeq 0.2$ and about 5% at $S \simeq 0.8$.

It is now possible to deduce a coverage scale $N(t)$ from the experimental value of $S(t)$ and the known incident beam flux I:

$$N(t) = I \int_0^t S(t) \, dt . \qquad (4.1)$$

The result is indicated at the top of Figs. 5 and 6, with error bars corresponding to the uncertainty in $S(t)$. In the above equation, I is calculated from the source pressure and temperature and the geometry of the apparatus with an accuracy estimated at $< 20\%$. This is verified by comparing the time scale of Fig. 2 with the
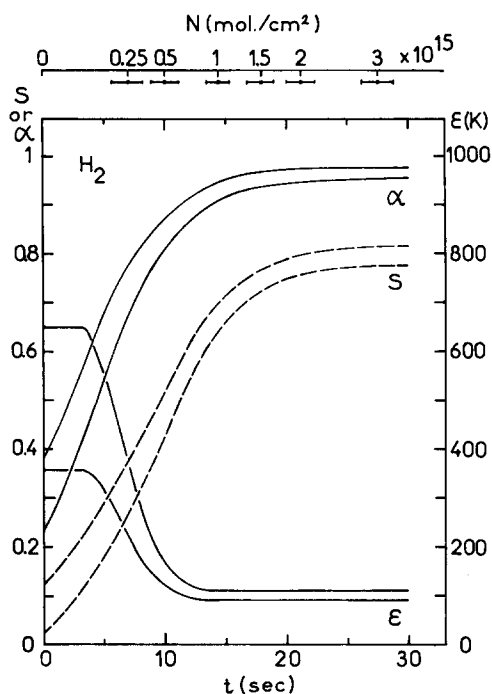
FIG. 5. Upper and lower bounds to S (- -) and α (—) obtained from the H_2 data of Fig. 2 when ϵ is allowed to vary between the limits shown [$n_1 = 3$, $n_2 = 5$, $360 \leq \epsilon_0 \leq 650$ K and $95 \leq \epsilon \leq 115$ K in Eq. (3.11)]. These bounds include the uncertainty due to a possible 10% error in the measurements of the MS signal $q_2(t)$. The upper abscisa shows the H_2 coverage calculated from Eq. (4.1).

analogous result of Schutte et al.,[9] whose beam flux is $\simeq 2$ times lower than ours.

Equation (4.1) neglects spontaneous evaporation, i.e., it assumes that molecules that "stick" on the surface for a time long compared to half the beam modulation period (definition of S, Sec. III. B) evaporate at a rate ($N \times 1/\tau$ per unit surface) which is low compared to the sticking rate $I \times S$. As mentioned in Sec. III. C, this may not be the case when $\epsilon \simeq 95$ K, the lower limit for the considered values of $\epsilon_\infty(H_2)$.[24] The determination of S through the MS measurements of the "reflected" molecules does ensure that one accounts for the possibility for weakly bound molecules to be "kicked off" by the incoming beam particles.

Qualitatively, the most striking feature of Figs. 5 and 6 is that the strong initial changes in the bolometer signal—and thus in α, S, and ϵ—in fact correspond to quite small changes in surface coverage. If we accept the traditional figure of $N_0 = 10^{15}$ molecules per "monolayer," we find that, starting from a H_2-free surface, the "break" in the bolometer signal (Figs. 2 and 3) corresponds to the adsorption of about 1/4 monolayer of hydrogen. At this point, $\alpha(H_2)$ has already increased by more than a factor of 2, while the adsorption of one additional monolayer is sufficient to bring $\alpha(H_2)$ to within $\simeq 10\%$ of its final value. For $S(H_2)$, the initial change is even more drastic—a factor $\simeq 4$ increase per $\simeq 1/4$ monolayer. The behavior of α (D_2) and S (D_2) is similar to that relative to H_2. We note that these considerations are based on a value of the beam flux per unit macro-

scopic area. If the exposed surface were significantly larger because of irregularities at the microscopic level, the effective flux would be lower, and we would have to conclude that the above changes in α and S occur over an even smaller coverage change.

The changes in ϵ with the surface coverage are more difficult to evaluate accurately, as our analysis does not depend critically on this parameter. However, independent measurements, in which a pure H beam is used to probe the amount of H_2 adsorbed on the surface, show that at a slightly higher surface temperature of $T_s = 3.5$ K, spontaneous evaporation occurs within about 2 min for coverages beyond $N/N_0 \simeq 0.5$. This means that for such a small coverage, $\epsilon(H_2)$ has already decreased to about 120 K, approaching the high-coverage limit of $\epsilon_\infty \simeq \epsilon_s = 103$ K, a behavior consistent with the shape of $\epsilon(t)$ in Figs. 5 and 6.

This conclusion agrees with the observation of Schutte et al.[9] that for surface temperatures $T_s > 6$ K the signal E on their first bolometer levels off around the first break in the E vs t plot (cf. Figs. 2 and 3). In this region, ϵ/T_s becomes small enough for the spontaneous evaporation rate to balance the beam arrival rate: hydrogen no longer accumulates, and α, S, and ϵ remain constant.

We conclude that α, S, and also ϵ change drastically when < 0.5 "monolayers" of hydrogen are adsorbed on the surface, and that a few additional layers are sufficient to ensure that the incoming beam particles no longer "see" the underlying cryodeposit. We also note
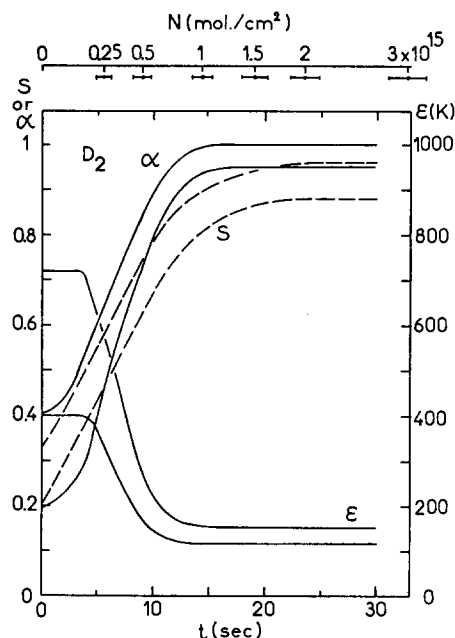

FIG. 6. Upper and lower bounds to S (- -) and α (—) obtained from the D_2 data of Fig. 3. In the representation of ϵ [Eq. (3.11), $n_1 = 3$, $n_2 = 5$], ϵ_0 was scaled to the limiting values estimated for H_2, while the limits to ϵ_∞ were estimated by the requirement $\alpha_\infty (D_2) \simeq \alpha_\infty (H_2)$: $400 \leq \epsilon_\infty \leq 720$ K, $116 \leq \epsilon_\infty \leq 156$ K. Allowance was made for a possible 10% error in the measurements of the MS signal $q_4(t)$. The upper abscisa shows the D_2 coverage calculated from Eq. (4.1).

that any preferential adsorption sites accessible at short exposure times would imply higher ϵ_0 values that those considered in Table II, resulting in lower values for α_0 and S_0 and even more pronounced variations than those indicated in Figs. 5 and 6.

The strong variation of α and S with surface composition was already noted by Brackmann and Fite,[7] but a quantitative comparison with their data is not possible, particularly as the amount of H_2 adsorbed on their substrate is not known. Schutte et al.[9] concluded from their experiments that at high (> 3 monolayers) H_2 coverage, S and α are near unity, while for $T_s \leqslant 4.25$ K a value $E_\infty(H_2) = 821$ K, very close to our value of 802 K, was obtained through an independent energy calibration of their bolometers which assumed $S_0 \simeq 0.2$ ($\alpha_0 \simeq 0.5$). These results are in agreement with the present data, considering that a small amount of H_2 remained on their surface at $t = 0$.

High values for the sticking coefficient on hydrogen covered surfaces have been obtained from pumping speed measurements by Hengevoss and Trendelenburg[25] ($T_s = 4.2$ K, $S \simeq 0.8$) and by Chubb and Pollard[26] ($T_s = 3.5-3.7$ K, $S \simeq 0.9$). These experiments may overestimate S, however, because the gas molecules can undergo more than one collision with the cold surface.

Changes in ϵ with surface coverage have been reported from thermal desorption measurements by Lee[19] and by Erents and Mc Cracken.[27] Lee finds ϵ for H_2 on H_2O ice to lie between 800 and 900 K for coverages < 1 monolayer of H_2, while $\simeq 10$ monolayers give $\epsilon \simeq 450$ K and > 50 monolayers give $\epsilon \simeq 100$ K. Admittedly, the coverage scale is only approximate, and the present data indeed suggest that ϵ decreases much more rapidly, unless the incoming beam particles would see an underlying substrate of pure H_2O ice much longer than the mixed cryodeposit in our experiments. This is unlikely, since Schutte et al.[9] found that adsorption of H_2O on their bolometer did not significantly change the H_2 coverage effect. Erents and McCracken report an average $\epsilon(H_2)$ of 96 K for > 10 monolayers of H_2 adsorbed on copper, and $\epsilon(H_2) = 126$ K for < 10 monolayers; for D_2 the corresponding values are 143 and 176 K, respectively. The average value for low H_2 coverage is substantially lower than that of Lee, but a closer specification of the coverage would be necessary for a meaningful comparison with our findings (assuming that the background cryodeposits are similar in both experiments).

We have calculated $\alpha(H_2)$ and $S(H_2)$ for a surface made up of CO_2, H_2O, or H_2 using the model proposed by Hollenbach and Salpeter.[16] These calculations do predict a low ($S \simeq 0.2$) sticking probability on CO_2 or H_2O and a higher value on $H_2(S \simeq 0.4)$, but the latter value is definetely too low. For α the trend is similar, but the absolute values are again smaller than our experimental results indicate: 0.1 and 0.2 for CO_2 and H_2O, 0.3 for H_2. As pointed out by the authors, their model is a purely classical one, however. The wavelength associated with the incoming hydrogen is about 1 Å in our experiments, which is comparable to the surface lattice

spacing, implying that a classical treatment cannot be expected to be quantitatively reliable.

A few final comments can be made with regard to the hydrogen adsorption on interstellar grains. The surface of these grains is covered with a cryodeposit of heavy molecules which should show a behavior towards impinging hydrogen molecules (or atoms) quite similar to that on the bolometer surface in the present experiments. Molecular hydrogen will condense on the grains until the binding energy becomes sufficiently low for the evaporation rate to balance the arrival rate. At a "typical" density $n_{H_2} \simeq 10^4$ cm^{-3} and gas temperature $\simeq 100$ K,[28] this occurs when $\epsilon \simeq 50 T_g$, where T_g is the grain temperature. For $T_g \simeq 10$ K, H_2 will therefore stop accumulating once $\epsilon \simeq 500$ K. According to our results and those of Schutte et al. (cf. the 10 K data in Fig. 5 of Ref. 9), the amount of H_2 adsorbed will remain quite low at such grain temperatures: $N/N_0 \simeq 0.2$. For D_2 on D_2 the sticking coefficient which we obtained for such coverage is < 0.5, for H_2 on H_2 it is < 0.3, and for H on H_2 it is lower yet. Lowering the gas temperature to the 100 K value appropriate to Hi clouds, is expected to increase S by less than 10% for binding energies around 500 K.[16,26] Hence, sticking coefficients below 0.3 will have to be assumed in evaluating the overall efficiency of hydrogen recombination at grain temperatures $T_g \gtrsim 10$ K.

ACKNOWLEDGMENTS

APPENDIX: JUSTIFICATION OF THE BOLOMETER CALIBRATION

Suppose that even at asymptotic H_2 coverage the two bolometers used by Schutte et al.[9] detected only a fraction β of all available energy, i.e. (Sec. III. C),

$$E_{1\infty} + E_{2\infty} = \beta[0.97(724 + \epsilon_\infty)] . \tag{A1}$$

As the second bolometer receives slower molecules (which should have higher α and $S^{16,26}$), a lower limit to the energy detected on the second bolometer is obtained by adopting the same S_∞ and α_∞ as for the first, so that [cf. Eq. (3.2)]

$$\{(724 + \epsilon_\infty) S_\infty + 721(1 - S_\infty)\alpha_\infty\} + (1 - S_\infty)\{[(1 - \alpha_\infty)$$

$$724 + \epsilon_\infty]S_\infty + 721\alpha_\infty(1 - \alpha_\infty)(1 - S_\infty)\} < \beta[0.97(724 + \epsilon_\infty)].$$
$$\tag{A2}$$

The first term in curly brackets refers to the first bolometer and the second term to the bolometer detecting the reflected molecules.

Our measurements yield [Eq. (3.4) and Fig. 2]

$$q_\infty = 1.05 \pm 0.1 = (1 - S_\infty)(1 - \gamma\alpha_\infty)^{-1/2} , \tag{A3}$$

where the uncertainty quoted allows for the reproducibility of the measurements (± 0.03) and the possible error

in the geometrical factor entering Eq. (4.2) through Eq. (3.7).

It can be verified that, allowing for the experimental uncertainty on q_∞ and a variation in ϵ_∞ from 95 to 115 K, Eqs. (A2) and (A3) can be satisfied simultaneously only if $\beta = 0.98-1$, which justifies the assumption on which the bolometer calibration was based.

[1] R. J. Gould and E. E. Salpeter, Astrophys. J. 138, 393 (1963).

[2] D. Hollenbach and E. E. Salpeter, Astrophys. J. 163, 155 (1971).

[3] D. J. Hollenbach, M. W. Werner, and E. E. Salpeter, Astrophys. J. 163, 165 (1971).

[4] H. D. Watson, Acc. Chem. Res. 10, 221 (1977).

[5] W. C. Stwalley, Phys. Rev. Lett. 37, 1628 (1976).

[6] A. J. Berlinsky, R. D. Etters, V. V. Goldman, and I. Silvera, Phys. Rev. Lett. 39, 356 (1977).

[7] R. T. Brackman and W. L. Fite, J. Chem. Phys. 34, 1572 (1961).

[8] G. Marenco, A. Schutte, G. Scoles, and F. Tommasini, J. Vac. Sci. Tech. 9, 824 (1972).

[9] A. Schutte, D. Bassi, F. Tommasini, A. Turelli, G. Scoles, and L. J. F. Hermans, J. Chem. Phys. 64, 4135 (1976).

[10] T. R. Govers, L. Mattera, and G. Scoles (to be published).

[11] M. Cavallini, G. Gallinaro, and G. Scoles, Z. Naturforsch. Teil A 22, 413 (1967).

[12] The accommodation coefficient α may in fact be different for translational and internal energy, but no information is available to allow a meaningful distinction.

[13] Throughout this paper, energy values are devided by Boltzmann's constant and expressed in Kelvin.

[14] A. Farkas, Ortho-hydrogen, Para-hydrogen, and Heavy-hydrogen (Cambridge University, Cambridge, England, 1935).

[15] H. Landolt and R. Börnstein, Zahlenwerte und Funktionen, edited by K. Schäfer and E. Lax (Springer, Berlin, 1961), Vol. II-4.

[16] D. Hollenbach and E. E. Salpeter, J. Chem. Phys. 53, 79 (1970).

[17] W. A. Steele, The Interaction of Gases with Solid Surfaces, The International Encyclopedia of Physical Chemistry and Chemical Physics, Topic 14, edited by D. H. Everett (Pergamon, Oxford, 1974), Vol. 3.

[18] G. F. J. Duquette, Ph.D. thesis, University of Waterloo (1977).

[19] T. J. Lee, Nature (London) Phys. Sci. 237, 99 (1972).

[20] V. B. Yuferov and F. I. Busol, Z. Tekh. Fiz. 36, 2042 (1966) [English translation Sov. Phys. Tech. Phys. 11, 1518 (1967)].

[21] D. R. O'Keefe, J. N. Smith Jr., R. L. Palmer, and H. Saltsburg, J. Chem. Phys. 52, 4447 (1970).

[22] L. Mattera, F. Rosatelli, C. Salvo, F. Tommasini, U. Valbusa, and G. Vidali, Surf. Sci. 93, 515 (1980).

[23] A. van Itterbeek, R. Hellemans, and W. van Dael, Physica (Utrecht) 31, 709 (1965).

[24] We notice that if $\epsilon_\infty = 103$ K, then $I \times S \simeq 15$ N/τ while for $\epsilon_\infty = 115$ K, $I \times S \simeq 10^3$ N/τ. It seems then reasonable that in our experimental conditions H_2 keeps accumulating on the surface.

[25] J. Hengevoss and E. A. Trendelenburg, Z. Naturforsch. Teil A 18, 481 (1963).

[26] J. N. Chubb and I. E. Pollard, Vacuum 15, 491 (1966).

[27] K. Erents and G. M. McCracken, Vacuum 21, 257 (1972).

[28] W. D. Watson, Rev. Mod. Phys. 48, 513 (1976).